

Surface-plasmon-enhanced light emitters based on InGaN quantum wells

KOICHI OKAMOTO¹, ISAMU NIKI^{1,2}, ALEXANDER SHVARTSER¹, YUKIO NARUKAWA², TAKASHI MUKAI² AND AXEL SCHERER^{1*}

¹Department of Electrical Engineering, California Institute of Technology, Pasadena, California 91125, USA

²Nitride Semiconductor Research Laboratory, Nichia Corporation, 491 Oka, Kaminaka, Anan, Tokushima, 774-8601, Japan

*e-mail: etcher@caltech.edu

Published online: 22 August 2004; doi:10.1038/nmat1198

Since 1993, InGaN light-emitting diodes (LEDs) have been improved and commercialized^{1,2}, but these devices have not fulfilled their original promise as solid-state replacements for light bulbs as their light-emission efficiencies have been limited³. Here we describe a method to enhance this efficiency through the energy transfer between quantum wells (QWs) and surface plasmons (SPs). SPs can increase the density of states and the spontaneous emission rate in the semiconductor³⁻⁹, and lead to the enhancement of light emission by SP-QW coupling^{10,11}. Large enhancements of the internal quantum efficiencies (η_{int}) were measured when silver or aluminium layers were deposited 10 nm above an InGaN light-emitting layer, whereas no such enhancements were obtained from gold-coated samples. Our results indicate that the use of SPs would lead to a new class of very bright LEDs, and highly efficient solid-state light sources.

Surface plasmons, excited by the interaction between light and metal surfaces¹²⁻¹⁵ are known to enhance absorption of light in molecules¹⁶ and increase Raman scattering intensities^{17,18}. Since 1990, SPs have also received much attention when used in LEDs³⁻⁹. Although coupling of spontaneous emission from InGaN QWs into the SP modes of thin, silver films was indirectly observed through increased absorption at the SP frequency¹⁰, and time-resolved measurements confirm that the recombination rate in QWs can be significantly increased¹¹, light has not yet been efficiently extracted from SP-enhanced InGaN emitters at visible wavelengths. Here we report large photoluminescence (PL) increases from InGaN/GaN QW material coated with metal layers. By polishing the bottom surface of sapphire-substrate-grown InGaN samples, QW emission can be photoexcited and measured through the back of the substrate, permitting the rapid comparison between PL from QWs in proximity with different metal coatings and at different distances from the metal film (Fig. 1a).

Figure 1b shows typical luminescence spectra from an InGaN/GaN QWs separated from silver, aluminium and gold layers by 10 nm GaN spacers. For Ag coatings, the luminescence peak of the uncoated wafer at 470 nm is normalized to 1, and a 14-fold enhancement in peak PL intensity is observed from the Ag-coated emitter. The luminescence intensity integrated over the emission spectrum is increased by 17 times, whereas eightfold peak intensity and sixfold integrated intensity enhancements are obtained from Al-coated InGaN QW. The PL is not

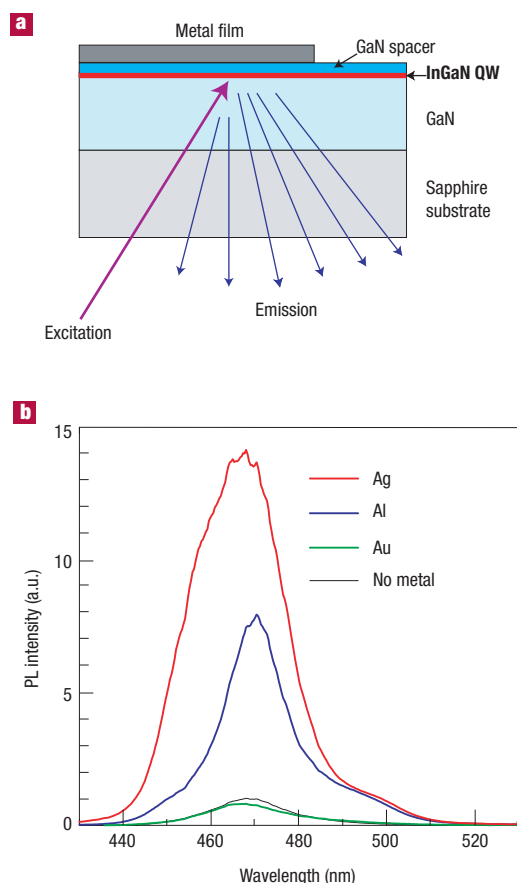


Figure 1 Photoluminescence measurements. **a**, Sample structure and excitation/emission configuration of PL measurement. **b**, PL spectra of InGaN/GaN QWs coated with Ag (red line), Al (blue line) and Au (green line). a.u. - arbitrary units. The distance between the metal layers and QWs was 10 nm. The PL peak intensity of uncoated InGaN/GaN QW (black line) at 470 nm was normalized to 1.

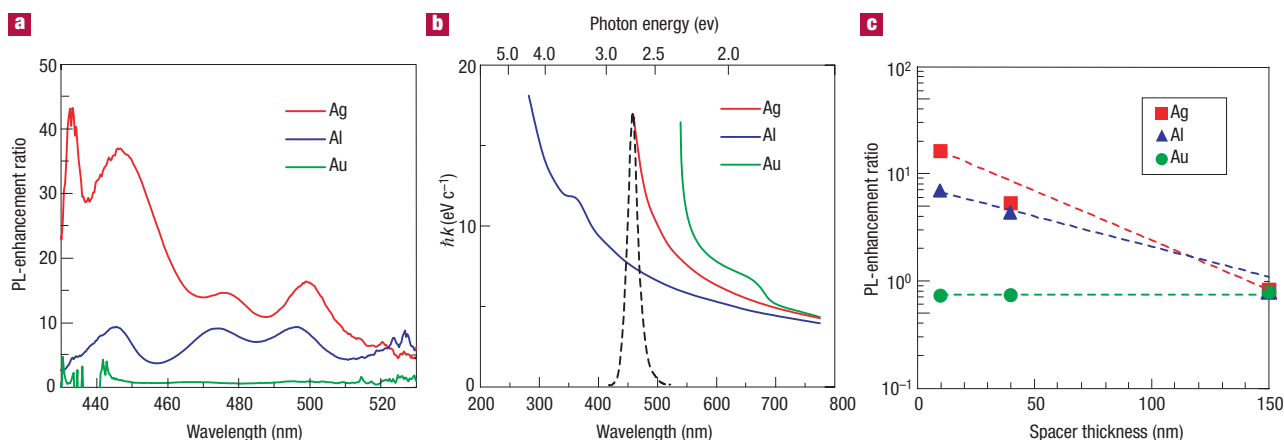


Figure 2 PL enhancement ratios. **a**, PL enhancement ratios at several wavelengths for the same samples as Fig. 1b. **b**, Dispersion diagrams of surface plasmons generated on Ag/GaN (red line), Al/GaN (blue line) and Au/GaN (green line) surfaces. k is the SP wave vector. The dashed line is the PL spectrum of InGaN/GaN. **c**, Integrated PL enhancement ratios for samples with Ag (red square), Al (blue triangle), and Au (green circle) are plotted against the thicknesses of GaN spacers. The dashed lines are the calculated penetration depths.

increased after Au coating. A small increase in the luminescence intensity might be expected after metallization because the metal reflects pump light back through the QW, doubling the effective path of the incident light, but differences between Au and Ag reflectivities at 470 nm cannot explain the large difference in the measured enhancement alone.

Figure 2a shows the enhancement ratios of PL intensities with metal layers separated from the QWs by 10 nm spacers as a function of wavelength. We find that the enhancement ratio increases at shorter wavelengths for Ag samples, whereas it is independent of wavelength for Al-coated samples. The PL enhancement after coating with Ag and Al can be attributed to strong interaction with SPs. Electron–hole pairs excited within the QW couple to electron vibrations at the metal/semiconductor interface when the energies of electron–hole pairs in InGaN ($\hbar\omega_{\text{InGaN}}$) and of the metal SP ($\hbar\omega_{\text{SP}}$) are similar, where \hbar and ω are the reduced Planck constant and the frequency, respectively. Then, electron–hole recombination produce SPs instead of photons, and this new recombination path increases the spontaneous recombination rate.

Figure 2b shows the dispersion diagrams of SP on metal/GaN surfaces calculated from reported dielectric functions^{19–22}. The plasmon energy ($\hbar\omega_{\text{p}}$) of silver is 3.76 eV (ref. 19), but this energy must be modified for Ag/GaN surface coatings to $\hbar\omega_{\text{SP}} \approx 3$ eV (≈ 410 nm) when using the dielectric constant of Ag (ref. 19) and GaN (ref. 20). Thus, Ag is suitable for SP coupling to blue emission, and we attribute the large increases in luminescence intensity from Ag-coated samples to such resonant SP excitation. In contrast, the estimated $\hbar\omega_{\text{SP}}$ of gold on GaN is below ~ 2.2 eV (~ 560 nm)²¹, and no measurable enhancement is observed in Au-coated InGaN emitters as the SP and QW energies are not matched. In the case of Al, the $\hbar\omega_{\text{SP}}$ is higher than ~ 5 eV (~ 250 nm)²², and the real part of the dielectric constant is negative over a wide wavelength region for visible light. Thus, a substantial and useful PL enhancement is observed in Al-coated samples, although the energy match is not ideal at 470 nm and a better overlap is expected at shorter wavelengths. The clear correlation between Fig. 2a and b suggests that the obtained emission enhancement with Ag and Al is due to SP coupling.

PL intensities of Al- and Ag-coated samples were also found to depend strongly on the distance between QWs and the metal layers, in contrast to Au-coated samples. Figure 2c compares integrated PL enhancement ratios for three different GaN spacer thicknesses (of 10, 40, and 150 nm) for Ag, Al and Au coatings. Al and Ag samples show

exponential increases in the luminescence intensity as the spacer thickness is decreased, whereas no such improvement was measured in Au-coated QWs. This spacer-layer dependence of the PL enhancement ratios matches our models of SP–QW coupling, as the SP is an evanescent wave that exponentially decays with distance from the metal surface. Only electron–hole pairs located within the near-field of the surface can couple to the SP mode, and this penetration depth (Z) of the SP fringing field into the semiconductor is given by $Z = \lambda/2\pi[(\epsilon'_{\text{GaN}} - \epsilon'_{\text{metal}})/\epsilon'_{\text{metal}}]^2$ where ϵ'_{GaN} and ϵ'_{metal} are the real parts of the dielectric constants of the semiconductor and metal, and Z can be calculated as $Z = 47, 77$, and 33 nm for Ag, Al and Au, respectively. Figure 2c shows a good agreement between these calculated penetration depths (dashed lines) and measured values of the PL enhancement (symbols) for Ag and Al coated samples.

If the metal/semiconductor surface were perfectly flat, it would be difficult to extract light from the SP mode, a non-propagating evanescent wave. However, roughness and imperfections in evaporated metal coatings can efficiently scatter SPs as light. Such roughness in the metal layer was observed from topographic images obtained by shear-force microscopy of the original GaN surface (Fig. 3a) and the Ag-coated surface (Fig. 3b). Figure 3c,d shows the depth profile along the dashed lines in Fig. 3a,b, respectively. We measured a modulation depth of the Ag surface of approximately 30–40 nm whereas the GaN surface roughness was below 10 nm. Higher-magnification scanning electron microscopy (SEM) images of the Ag and GaN surfaces are shown in Fig. 3e,f. The length scale of the roughness of the Ag surface was determined to be a few hundred nanometres. Figure 3g shows a fabricated metal grating, a geometry that has previously been used to couple SP and photons^{3,5–8}. Microluminescence images of uncoated, coated and patterned grating structures of Ag on InGaN QWs with 10 nm spacers are shown in Fig. 3h. We found a doubling of the emission from 133-nm-wide Ag stripes forming a 400 nm period grating, whereas such an emission increase was not observed from 200-nm-wide Ag stripes within a 600 nm period grating. This measurement suggests that the size of the metal structure determines the SP–photon coupling and light extraction.

As spontaneous emission rates are increased, so are the internal quantum efficiencies, η_{int} . The external quantum efficiencies (η_{ext}) of light emission is given by the light-extraction efficiency (C_{ext}) and η_{int} , which is given by the ratio of the radiative (k_{rad}) and non-radiative (k_{non}) recombination rates of electron–hole pairs:

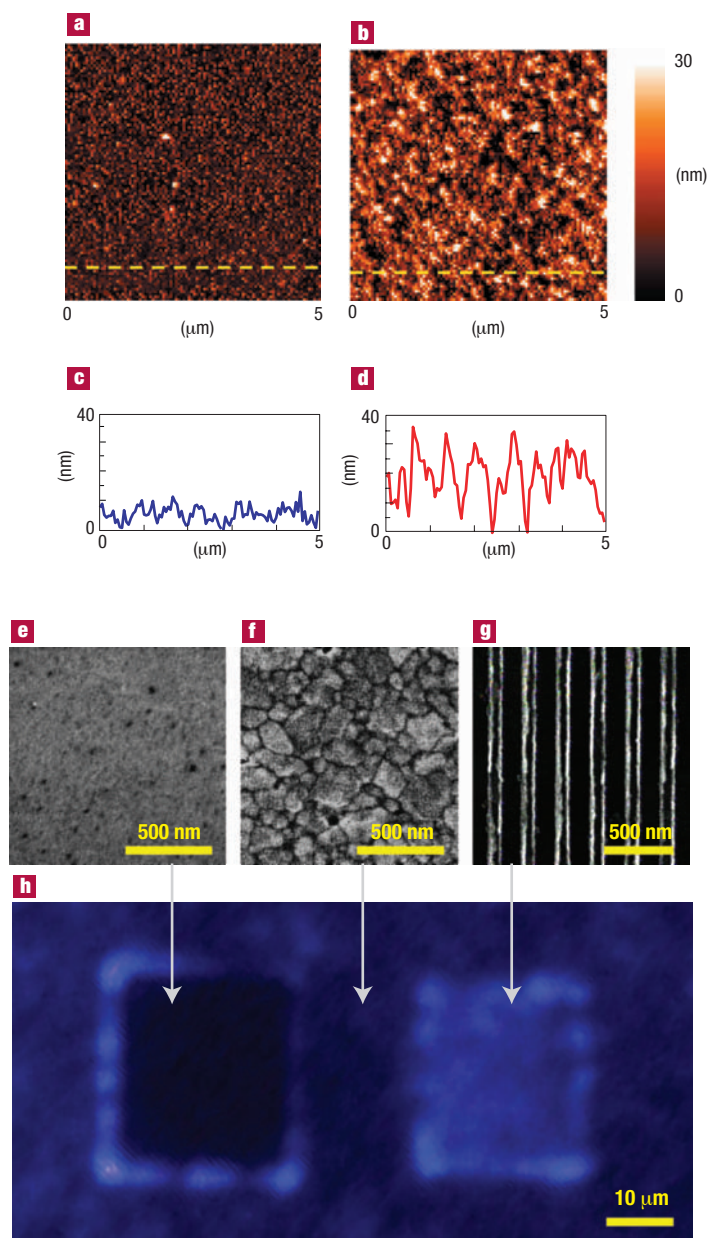


Figure 3 Topographic and luminescence images. **a**, Topographic image of the uncoated GaN surface. **b**, Topographic image of a 50-nm-thick Ag film evaporated on GaN. **c**, The depth profile along the dashed line in Fig. 3a. **d**, The depth profile along the dashed line in Fig. 3b. **e**, SEM image of the uncoated GaN surface. **f**, SEM image of the 50 nm Ag film evaporated on GaN. **g**, SEM image of the grating structure with 33% duty cycle fabricated within a 50-nm-thick Ag layer on GaN. **h**, Microluminescence image including the areas of **e–g**. All samples used were coated onto InGaN/GaN QWs with 10 nm GaN spacers.

$$\eta_{\text{ext}} = C_{\text{ext}} \times \eta_{\text{int}} = C_{\text{ext}} \times \frac{k_{\text{rad}}}{k_{\text{rad}} + k_{\text{non}}} \quad (1)$$

In order to obtain the η_{int} to separate the SP enhancement from other possible effects, we have measured the temperature dependence of the PL intensity. Figure 4a shows Arrhenius plots of the integrated PL intensities from InGaN QWs separated from Ag and Al films by 10 nm spacers, and compares these to uncoated samples. η_{int} values from uncoated QWs were estimated as 6% at room temperature by assuming $\eta_{\text{int}} \approx 100\%$ at 4.2 K (ref. 23). These η_{int} values increased 6.8 times (to 41%) after Ag coating and 3 times (to 18%) after Al coating, explainable

by spontaneous recombination rate enhancements through SP coupling. The 6.8-fold increasing of η_{int} means that 6.8-fold improvement of the efficiency of electrically pumped LED devices should be achievable because η_{int} is a fundamental property and does not depend on the pumping method. Such improved efficiencies of the white LEDs, in which a blue LED is combined with a yellow phosphor, are expected to be larger than those of current fluorescent lamps or light bulbs. The luminous efficacy of commercial white LEDs is 25 lm W^{-1} under a current of 20 mA at room temperature²⁴. This value is still lower than that of fluorescent tubes (75 lm W^{-1}). A threefold improvement is necessary to exceed the current fluorescent lamps or light bulbs.

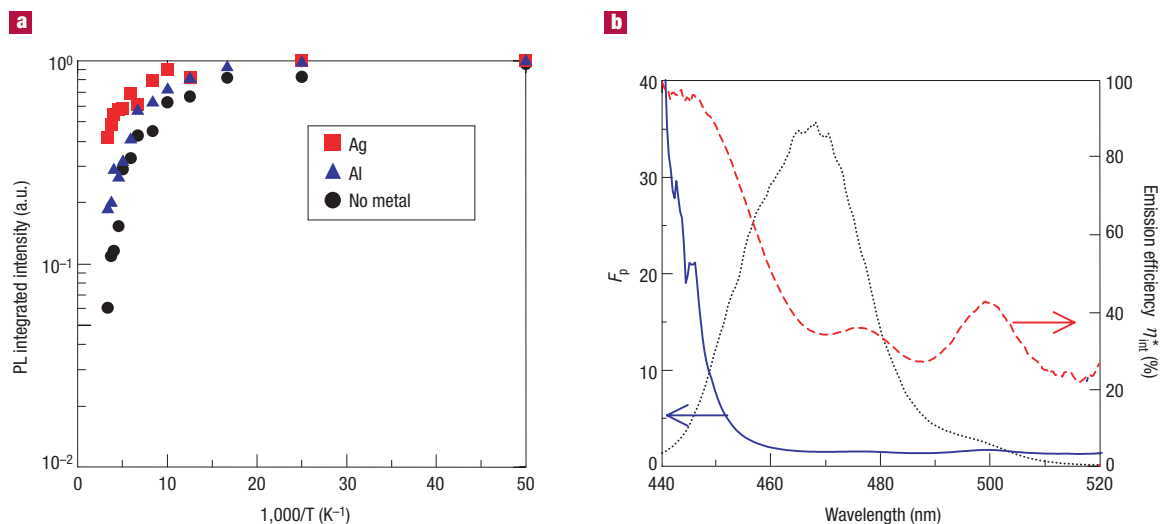


Figure 4 Temperature dependence and Purcell enhancement factors. **a**, Arrhenius plots of the integrated PL intensities of InGaN/GaN QWs with Ag (red square), Al (blue triangle) and uncoated sample (black circle) with 10 nm GaN spacers. PL integrated intensities at 4.2 K were normalized to 1. **b**, Wavelength-dependent emission efficiencies ($\eta_{\text{int}}^*(\omega)$) of the InGaN/GaN with Ag layer with 10 nm GaN spacers (red dashed line). The Purcell enhancement factor $F_p(\omega)$ estimated by $\eta_{\text{int}}^*(\omega)$ was also plotted (blue solid line). The dotted black line is the PL spectrum of the same sample.

We expect that the SP coupling technique is very promising for even larger improvements of solid-state light source.

Wavelength-dependent enhanced efficiencies $\eta_{\text{int}}^*(\omega)$ can be related to the coupling rate $k_{\text{SP}}(\omega)$ between QWs and SPs by the relationship:

$$\eta_{\text{int}}^*(\omega) = \frac{k_{\text{rad}}(\omega) + C'_{\text{ext}}(\omega)k_{\text{SP}}(\omega)}{k_{\text{rad}}(\omega) + k_{\text{non}}(\omega) + k_{\text{SP}}(\omega)} \quad (2)$$

where $C'_{\text{ext}}(\omega)$ is the probability of photon extraction from the SP's energy, and is decided by the ratio of the light scattering and dumping of electron vibration. $C'_{\text{ext}}(\omega)$ depends on the roughness and structure of the metal surface (Fig. 3h). Figure 4b shows the $\eta_{\text{int}}^*(\omega)$ of Ag-coated sample estimated from the PL-enhancement ratio (Fig. 2a) by normalizing the integrated η_{int}^* should be 41%. We find that $\eta_{\text{int}}^*(\omega)$ increases at shorter wavelengths where the plasmon resonance more closely matches the QW emission, and reaches almost 100% at 440 nm. The Purcell enhancement factor²⁵ F_p quantifies the increase in spontaneous emission rate into a mode of interest, and can be described by $\eta_{\text{int}}(\omega)$ and $\eta_{\text{int}}^*(\omega)$ when $C'_{\text{ext}} \approx 1$:

$$F_p(\omega) = \frac{k_{\text{rad}}(\omega) + k_{\text{non}}(\omega) + k_{\text{SP}}(\omega)}{k_{\text{rad}}(\omega) + k_{\text{non}}(\omega)} \approx \frac{1 - \eta_{\text{int}}(\omega)}{1 - \eta_{\text{int}}^*(\omega)} \quad (3)$$

Figure 4b also shows $F_p(\omega)$ estimated at each wavelength by assuming a constant $\eta_{\text{int}}(\omega) = 6\%$. $F_p(\omega)$ is significantly higher at wavelengths below 460 nm, well in agreement with previous work^{10,11}. The PL spectrum shape, plotted as a black dotted line, also indicates that $F_p(\omega)$ values are higher for shorter wavelengths, a possible reason for the asymmetry in the luminescence peak of Fig. 1b. Figure 4b suggests that InGaN QWs with peak positions around 440 nm should be matched with SPs from silver layers, yielding enhanced $\eta_{\text{int}}^*(\omega)$ approaching 100% throughout the luminescence spectrum. The SP could be geometrically tuned to match our $\lambda \approx 470$ nm QW by fabricating nanostructures (for example, using a grating structure^{3,5-8}).

The SP enhancement of InGaN QW emission provides a promising method for developing highly efficient solid-state light sources.

The significant η_{int} increases are due to higher spontaneous recombination rate, and the distance and choice of patterned metal films can be used to optimize light emitters. Even when using unpatterned metal layers, the SP energy can be extracted by the submicrometre-scale roughness on the metal surface. SP coupling is one of the most interesting methods for developing efficient LEDs, as the metal can be used both as an electrical contact and for exciting plasmons. We believe that this work provides the foundation for rapid development of highly efficient solid-state light emitters, not only limited to III-V materials.

METHODS

In_{0.3}Ga_{0.7}N QWs 3 nm thick were grown onto GaN (4 μm thick)/sapphire (0001) substrates by metal-organic chemical vapour deposition. To investigate the influence of the distance between the metal and the QW, 10, 40 and 150 nm thick GaN spacers were grown onto these QWs, and 50 nm thick Ag, Al or Au layers were then evaporated on top of the wafer surfaces (Fig. 1a). PL measurements were performed by exciting the QWs with a 406 nm diode laser (Edmond Industrial Optics) from the back of the substrates, and collecting luminescence with a multichannel spectrometer (Ocean Optics USB2000). The excitation power was 4.5 mW. The temperature dependence of the luminescence intensity was determined by cooling the samples in a cryostat (Oxford Microstat) to ~4.2 K during such measurements. Topographic measurements were performed by a twin near-field optical microscope system manufactured by OMICRON. Fluorescence microscopy (Olympus IX71) was used with ×40 objective, a mercury lamp, and a colour charge-coupled device camera. Metal grating structures were fabricated by electron-beam lithography on a 50-nm-thick polymethylmethacrylate mask coated on the 50-nm-thick Ag surface. Electron-beam lithography was performed in a converted Hitachi S-4500 field-emission SEM operated at 30 kV. The pattern was transferred through the top metal layer by argon-ion milling, resulting in 400 nm and 600 nm period gratings on InGaN/GaN QWs with 10 nm GaN spacers. The duty cycle of these silver gratings was ~33%.

Received 15 December 2003; accepted 19 July 2004; published 22 August 2004.

References

- Nakamura, S., Mukai, T. & Senoh, M. Candela-class high-brightness InGaN/AlGaIn double-heterostructure blue-light-emitting diodes. *Appl. Phys. Lett.* **64**, 1687–1689 (1994).
- Nakamura, S. & Fasol, G. *The Blue Laser Diode: GaN-Based Light Emitting Diode and Lasers* (Springer, Berlin, 1997).
- Köck, A., Gornik, E., Hauser, M. & Beinstling, W. Strongly directional emission from AlGaAs/GaAs light-emitting diode. *Appl. Phys. Lett.* **57**, 2327–2329 (1990).
- Hecker, N. E., Hopfel, R. A. & Sawaki, N. Enhanced light emission from a single quantum well located near a metal coated surface. *Physica E* **2**, 98–101 (1998).
- Hecker, N. E., Hopfel, R. A., Sawaki, N., Maier, T. & Strasser, G. Surface plasmon-enhanced photoluminescence from a single quantum well. *Appl. Phys. Lett.* **75**, 1577–1579 (1999).
- Barnes, W. L. Electromagnetic crystals for surface plasmon polaritons and the extraction of light from

- emissive devices. *J. Light. Tech.* **17**, 2170–2182 (1999).
7. Gianordoli, S. *et al.* Optimization of the emission characteristics of light emitting diodes by surface plasmons and surface waveguide modes. *Appl. Phys. Lett.* **77**, 2295–2297 (2000).
 8. Vuckovic, J., Loncar, M. & Scherer, A. Surface plasmon enhanced light-emitting diode. *IEEE J. Quant. Elec.* **36**, 1131–1144 (2000).
 9. Hobson, P. A., Wedge, S., Wasey, J. A. E., Sage, I. & Barnes, W. L. Surface plasmon mediated emission from organic light emitting diodes. *Adv. Mater.* **14**, 1393–1396 (2002).
 10. Gontijo, I. *et al.* Coupling of InGaN quantum-well photoluminescence to silver surface plasmons. *Phys. Rev. B* **60**, 11564–11567 (1999).
 11. Neogi, A. *et al.* Enhancement of spontaneous recombination rate in a quantum well by resonant surface plasmon coupling. *Phys. Rev. B* **66**, 153305 (2002).
 12. Ebbesen, T. W., Lezec, H. J., Ghasemi, H. F., Thio, T. & Wolff, P. A. Extraordinary optical transmission through sub-wavelength hole arrays. *Nature* **391**, 667–669 (1998).
 13. Schroter, U. & Heitmann, D. Surface-plasmon-enhanced transmission through metallic gratings. *Phys. Rev. B* **58**, 15419–15421 (1998).
 14. Kitson, S. C., Barnes, W. L. & Sambles, J. R. A full photonic band gap for surface modes in the visible. *Phys. Rev. Lett.* **77**, 2670–2673 (1996).
 15. Barnes, W. T., Preist, T. W., Kitson, S. C. & Sambles, J. R. Physical origin of photonic energy gap in the propagation of surface plasmon on grating. *Phys. Rev. B* **54**, 6227–6244 (1996).
 16. Ford, G. W. & Weber, W. H. Electromagnetic-interactions of molecules with metal-surfaces. *Phys. Rep.* **113**, 195–287 (1984).
 17. Fleischmann, M., Hendra, P. J. & McQuillan, A. J. Raman spectra of pyridine adsorbed at a silver electrode. *Chem. Phys. Lett.* **26**, 163–166 (1974).
 18. Garcia-Vidal, J. F. & Pendry, J. B. Collective theory for surface enhanced Raman scattering. *Phys. Rev. Lett.* **77**, 1163–1166 (1996).
 19. Liebsch, A. Surface plasmon dispersion of Ag. *Phys. Lev. Lett.* **71**, 145–148 (1993).
 20. Kawashima, T., Yoshikawa, H., Adach, S., Fuke, S. & Ohtsuk, K. Optical properties of hexagonal GaN. *J. Appl. Phys.* **82**, 3528–3535 (1997).
 21. Palik, E. D. *Handbook of Optical Constants of Solids* (Academic, San Diego, 1985).
 22. Bagchi, A., Duke, C. B., Feibelman, P. J. & Porteus, J. O. Measurement of surface-plasmon dispersion in aluminum by inelastic low-energy electron diffraction. *Phys. Rev. Lett.* **27**, 998–1001 (1971).
 23. Kawakami, Y. *et al.* Radiative and nonradiative recombination processes in GaN-based semiconductors. *Phys. Status Solidi A* **183**, 41–50 (2001).
 24. Narukawa, Y. *et al.* Phosphor-conversion white light emitting diode using InGaN near-ultraviolet chip. *Jpn J. Appl. Phys.* **37**, L371–L373 (2003).
 25. Purcell, E. M. Spontaneous emission probabilities at radio frequencies. *Phys. Rev.* **69**, 681–681 (1946).

Acknowledgements

The authors wish to thank the US Air Force Office for Scientific Research for their support under contract F49620-03-1-0418.

Correspondence and requests for materials should be addressed to A.S.

Competing financial interests

The authors declare that they have no competing financial interests.